# Twist Viscosity of Side-Chain Liquid-Crystalline Polysiloxanes in a Nematic Solvent

**Pei-Yuan Liu, Ning Yao, and Alex M. Jamieson***

*Department of Macromolecular Science Case, Western Reserve University, Cleveland, Ohio 44106-7202*

*Received March 16, 1999; Revised Manuscript Received July 26, 1999*

ABSTRACT: Electric-field-dependent dynamic light scattering (EFDLS) was used to determine the twist elastic constant and twist viscosity of miscible nematic solutions of side-chain liquid crystal polysiloxanes (SCLCP) in 4′-(pentyloxy)-4-cyanobiphenyl (5OCB). The results show that addition of SCLCP leads to a decrease in the twist relaxation rate, which derives mainly from an increase in twist viscosity. The magnitude of the twist viscosity increment varies with molecular weight and spacer length, proportional to changes in the molecular hydrodynamic volume of the polymer. These results are consistent with the Brochard model of the viscous loss introduced by the dissolved polymer, modified by inclusion of an additional dissipation mechanism, postulated to arise from an elastic torque between director rotation and LCP orientation.

## Introduction

Dissolution of liquid crystal polymers (LCPs) in low-molar-mass nematogens (LMMN) causes an increase in viscosity whose origin is similar to that which occurs in solutions of ordinary polymers in isotropic solvents.[1] However, in nematic solutions, the viscometric behavior is complicated by the fact that the solvent is anisotropic, and hence, a variety of distinct viscosity coefficients can be measured. A theoretical analysis by Brochard[1] predicts that, depending on its chain conformation (i.e., prolate vs oblate), the dissolved polymer may influence these viscosities differently. Several groups have investigated experimentally the viscometric properties of dilute solutions of an LCP in a nematic solvent.[2−15] Our own studies[4,7,9−15] have clearly demonstrated that the change in various viscosity coefficients of the nematic solvent depends not only on the hydrodynamic volume and molecular weight of the dissolved LCP but also on its molecular architecture (e.g., side-chain vs main-chain). In this paper, we focus on our observation[13−15] that a side-chain liquid crystalline polymer (SCLCP), dissolved in a flow-aligning nematic solvent such as 5CB ($\alpha_2\alpha_3 > 0$), alters the rheology to director-tumbling character ($\alpha_2\alpha_3 < 0$); i.e., the director is continuously rotated around the vorticity axis by the hydrodynamic torques. Here, $\alpha_2$ and $\alpha_3$ are two of the six Leslie viscosity coefficients that determine the orientational response of the nematic director.[16,17]

This observation was demonstrated by Gu et al.[13,14] to be qualitatively consistent with theoretical prediction by the molecular hydrodynamic model of Brochard[1] that provides expressions for the effect of dissolved polymer on various nematic viscosity coefficients. In particular, the predictions for the increments in the rotational and irrotational torque coefficients, $\gamma_1$ and $\gamma_2$, respectively, are[1]

$$\delta\gamma_1 = \left(\frac{ckT}{N}\right)\tau_R\frac{(R_\perp^2 - R_\parallel^2)^2}{R_\perp^2 R_\parallel^2} \tag{1}$$

$$\delta\gamma_2 = \left(\frac{ckT}{N}\right)\tau_R\frac{(R_\perp^4 - R_\parallel^4)}{R_\perp^2 R_\parallel^2} \tag{2}$$

where $c$ is the LCP concentration, $k$ is Boltzmann's constant, $T$ is the absolute temperature, $N$ is the degree of polymerization of the LCP, and $\tau_R$ represents the conformational relaxation time of the chain, which can be expressed in terms of the rms end-to-end distances ($R_\perp$ and $R_\parallel$) and the translational frictional coefficients ($\lambda_\perp$ and $\lambda_\parallel$) perpendicular and parallel, respectively, to the nematic director:

$$\tau_R = \left[\frac{\lambda_\perp\lambda_\parallel R_\perp^2 R_\parallel^2}{\lambda_\perp R_\perp^2 + \lambda_\parallel R_\parallel^2}\right]\left(\frac{1}{kT}\right) \tag{3}$$

Because $\alpha_2 = {}^1/_2(\gamma_2 - \gamma_1)$ and $\alpha_3 = {}^1/_2(\gamma_2 + \gamma_1)$,[14,17,18] eqs 1 and 2 lead to the following expressions for the increments in the Leslie viscosity coefficients:

$$\delta\alpha_2 = \left(\frac{ckT}{N}\right)\tau_R\left(\frac{R_\perp^2 - R_\parallel^2}{R_\perp^2}\right) \tag{4}$$

and

$$\delta\alpha_3 = \left(\frac{ckT}{N}\right)\tau_R\left(\frac{R_\perp^2 - R_\parallel^2}{R_\parallel^2}\right) \tag{5}$$

As indicated by eqs 4 and 5, a flow-aligning nematic ($\alpha_2\alpha_3 > 0$) such as 5CB or 5OCB is transformed to a flow-tumbling solution ($\alpha_2\alpha_3 < 0$) by dissolution of a sufficient amount of a side-chain LCP when $R_\perp > R_\parallel$. As a corollary, eqs 4 and 5 predict that addition of a main-chain LCP ($R_\parallel > R_\perp$) to a tumbling flow LMMN ($\alpha_2\alpha_3 < 0$) such as 8CB can produce a flow-aligning mixture ($\alpha_2\alpha_3 > 0$). This has also been confirmed experimentally.[14] Unfortunately, on more detailed examination of these experimental observations, certain discrepancies in relation to theory become apparent.[13,14] For example, eqs 4 and 5 predict that $\delta\alpha_2$ and $\delta\alpha_3$ should have the same signs for a particular ratio $R_\perp/R_\parallel$. This is in contradiction to experimental analysis[13,14] of the

* To whom all correspondence should be addressed.

10.1021/ma990389e CCC: $18.00 © 1999 American Chemical Society
Published on Web 09/04/1999

stress transients from tumbling solutions of side-chain LCPs, which indicate that these two quantities have opposite signs ($\delta\alpha_2 < 0$, $\delta\alpha_3 > 0$).

A second area of experimentation concerns the fact that dilute nematic solutions of LCPs exhibit a change in magnitude of the well-known[12,19,20] electrorheological (ER) effect. Specifically, on dissolving a main-chain LCP, the increment in shear viscosity with the field on ($\delta\eta_{on}$) is much larger than that with the field off ($\delta\eta_{off}$), i.e., $\delta\eta_{on} \gg \delta\eta_{off}$, and is strongly molecular weight-dependent. In contrast, the change in magnitude of the ER effect in solutions of side-chain LCPs is small, $\delta\eta_{on} \approx \delta\eta_{off}$, and is weakly molecular weight-dependent.[12,19,20] Again, these results are qualitatively consistent with the hydrodynamic theory of Brochard,[1] which leads to the following predictions for the Miesowicz viscosities.[16,17,21]

$$\delta\eta_b = \left(\frac{ckT}{N}\right)\tau_R\left(\frac{R_\perp^2}{R_\parallel^2}\right) \tag{6}$$

$$\delta\eta_c = \left(\frac{ckT}{N}\right)\tau_R\left(\frac{R_\parallel^2}{R_\perp^2}\right) \tag{7}$$

Taking the ratio of eqs 6 and 7, we have

$$\left(\frac{\delta\eta_c}{\delta\eta_b}\right) = \left(\frac{R_\parallel}{R_\perp}\right)^4 \tag{8}$$

By equating $\eta_{on} = \eta_c$ and $\eta_{off} = \eta_b$, eq 8 can be applied to interpret the effect of LCP molecular architecture on the ER behavior of LCP/LMMN solutions. Thus, dissolution of a main-chain LCP ($R_\parallel \gg R_\perp$) produces a large increase in ER response ($\delta\eta_{on}/\delta\eta_{off} \approx \delta\eta_c/\delta\eta_b \gg 1$) that is strongly molecular weight-dependent ($\delta\eta_{on}/\delta\eta_{off} \approx M$); dissolution of a side-chain LCP ($R_\parallel \approx R_\perp$) causes a small change in ER response ($\delta\eta_{on}/\delta\eta_{off} \approx \delta\eta_c/\delta\eta_b \approx 1$) that is weakly molecular weight-dependent ($\delta\eta_{on}/\delta\eta_{off} \approx M^{-0.3}$). Here, a further discrepancy between experiment and the Brochard model was pointed out by Yao and Jamieson.[22] It was observed that solutions of side-chain LCPs that exhibit tumbling flow, implying an oblate conformation ($\delta\alpha_3 > 0$, i.e., $R_\perp > R_\parallel$) (eq 5), show ER behavior ($\delta\eta_{on}/\delta\eta_{off} = \delta\eta_c/\delta\eta_b > 1$), indicative of a prolate conformation ($R_\parallel > R_\perp$) (eq 8).

As a result of these inconsistencies, a phenomenological modification of the Brochard model was proposed.[22] Brochard[1] considered the viscous dissipation introduced by dissolving a regular polymer in a nematic solvent. The analysis involves computing the torque $\Gamma$ on the director $\vec{\mathbf{n}}$ in a nematic medium:

$$\Gamma = \vec{\mathbf{n}}\times\left[\gamma_1\left(\frac{d\vec{\mathbf{n}}}{dt} - \vec{\omega}\cdot\vec{\mathbf{n}} + \gamma_2\vec{\mathbf{A}}\cdot\vec{\mathbf{n}}\right)\right. \tag{9}$$

where $\vec{\omega} = {}^1/_2\vec{\nabla}\times\vec{\mathbf{v}}$ is the antisymmetric velocity gradient tensor and $\vec{\mathbf{A}}$ is the symmetric velocity gradient tensor, $A_{\alpha\beta} = 1/2(\partial_\alpha v_\beta + \partial_\beta v_\alpha)$. Brochard[1] computed the contributions to $\Gamma_y$, the torque about the vorticity axis, from flows in the $xz$ plane. For a liquid crystal polymer, we propose that in the absence of a viscous flow an additional contribution to the torque can arise due to an elastic coupling between director rotation and the orientation of the LCP chain.[23] This torque contribution $\delta\Gamma_y^{el}$ produces viscous dissipation by causing rotation of the chain about the vorticity axis. The chain rotation is opposed by a frictional torque $\xi v$ where $\xi$ is the rotational frictional coefficient and $v = d\vec{\mathbf{n}}/dt$ is the rate of director rotation. In steady state, we have

$$\delta\Gamma_y^{el} = \delta\gamma_1^{el}\frac{d\vec{\mathbf{n}}}{dt} = \left(\frac{c}{N}\right)v\xi = \left(\frac{ckT}{N}\tau_{rot}\right)\frac{d\vec{\mathbf{n}}}{dt} \tag{10}$$

where $\delta\gamma_1^{el}$ is the additional contribution to the rotational viscosity and $\tau_{rot} = \xi/kT$ is the rotational relaxation time. Thus,

$$\delta\gamma_1^{el} = \left(\frac{ckT}{N}\right)\tau_{rot} \tag{11}$$

For quasispherical particles, we equate $\tau_{rot} = \tau_R$, and this leads[22] directly to a revised version of the Brochard expression for the twist viscosity increment:

$$\delta\gamma_1^{modified} = \delta\gamma_1^{Brochard} + \delta\gamma_1^{el} = \left(\frac{ckT}{N}\right)\tau_R\left[\frac{(R_\perp^2 - R_\parallel^2)^2}{R_\perp^2 R_\parallel^2} + 1\right] \tag{12}$$

and hence

$$\delta\alpha_2 = \left(\frac{ckT}{N}\right)\tau_R\left(\frac{1}{2} - \frac{R_\parallel^2}{R_\perp^2}\right) \tag{13}$$

$$\delta\alpha_3 = \left(\frac{ckT}{N}\right)\tau_R\left(\frac{R_\perp^2}{R_\parallel^2} - \frac{1}{2}\right) \tag{14}$$

Equations 12−14 lead to much better agreement with experiment because a flow-aligning to tumbling transition can now occur such that $\delta\alpha_3 > 0$ but $\delta\alpha_2 < 0$ when the LCP conformation is quasispherical, $R_\parallel \approx R_\perp$. In addition, because $\delta\eta_b$ and $\delta\eta_c$ do not involve director rotation and hence remain unchanged (viz., eqs 6 and 7), it becomes possible in this case to have both $\delta\alpha_3 > 0$ and $\delta\eta_c > \delta\eta_b$.

In the present paper, we are concerned with the fact that the modified theoretical model, as expressed in eq 12, predicts the increment in twist viscosity coefficient of nematic solutions of a quasispherical LCP ($R_\parallel \approx R_\perp$) is large ($\approx(ckT/N)\tau_R$) rather than approximately equal to zero, as indicated by the original equation (1). Of particular interest, therefore, is to further test the modified Brochard model by investigating the twist viscosity increment $\delta\gamma_1$ of side-chain SCLCP solutions. In this study, we characterize the viscoelastic behavior of a nematic monodomain having a polysiloxane SCLCP dissolved in a nematic solvent (5OCB), determining the twist viscosity, $\gamma_1$, and elastic constant, $K_{22}$, via the electric-field-dependent dynamic light scattering (EFDLS) technique. These results are compared with previous measurements of the Miesowicz viscosities, $\eta_c$ and $\eta_b$, on the same LCP solutions obtained by ER analysis. The effect of temperature, molecular weight, and spacer length on the twist viscosity increment is studied and discussed. The data are interpreted in terms of our modification of the theory of Brochard.[22]

## Experimental Section

**Materials.** The low-molar-mass nematic liquid crystal solvent 4′-(pentyloxy)-4-cyanobiphenyl (5OCB, $T_{NI} = 67$ °C) used in this study was purchased from Aldrich Chemical Co. The side-chain LCPs are derivatives of poly(methysiloxane)

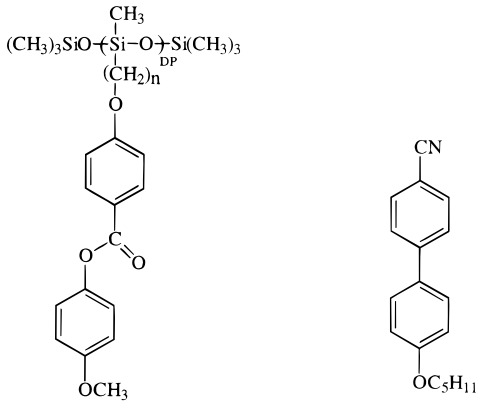


**Figure 1.** Chemical structures of the side-chain LCPs and 5OCB.

**Table 1. Values of DP, Spacer Length, and Molecular Weight of the Side-Chain Liquid Crystalline Polysiloxanes**

| sample | DP[a] | n[b] | $M_n$[c] | $M_w$[c] | $M_w/M_n$ |
|---|---|---|---|---|---|
| no. 1 | 45 | 3 | 9 600 | 13 500 | 1.41 |
| no. 2 | 72 | 3 | 11 800 | 22 200 | 1.88 |
| no. 3 | 198 | 3 | 16 600 | 40 300 | 2.42 |
| no. 4 | 198 | 5 | 12 400 | 21 200 | 1.71 |
| no. 5 | 198 | 11 | 13 100 | 33 300 | 2.54 |

[a] DP = degree of polymerization of the backbones based on H NMR analysis. [b] $n$ = spacer length of the side chains. [c] $M_n$ and $M_w$ were measured by GPC using THF as a solvent and polystyrene as a standard.

(DP = 45, 72, 198), where a mesogenic phenylbenzoate group is grafted to the main chain via a flexible methylene spacer of variable length, $n = 3, 5, 11$. The chemical structures of 5OCB and the side-chain LCPs are schematized in Figure 1. Each of the polymers has been extensively characterized.[12] Table 1 shows the data on number-average DP (degree of polymerization, measured via $^1$H NMR), spacer length ($n$), and GPC molecular weights for these side-chain LCPs. We point out that for the polymers having DP = 198 there is a minimum in GPC molecular weight at spacer length $n = 5$. As described in a previous work,[12] this indicates that there is a minimum in hydrodynamic volume at $n = 5$, which will be a focal point of later discussion. All materials were used as received without further purification.

A small amount of the polymer in 5OCB was heated at a temperature above its clearing transition and ultrasonically agitated to make a homogeneous, miscible mixture. Equilibration was continued at least 24 h until complete dissolution in the isotropic state. Homeotropic monodomains, in which the average molecular orientation of the director is perpendicular to the glass surfaces, were formed between ITO conductive glass slides coated with a 0.35 wt % solution of lecithin in ethanol, purchased from Sigma Chemical Company. The thickness of the scattering cell was controlled by 12.5 $\mu$m Mylar spacers, and the cells were sealed with epoxy resin (DEVCON). The sample cell thickness was measured by interferometry[24,25] with values accurate to within 1%. Cells were filled with the isotropic mixtures at a temperature around 75 °C via capillary action on a hot stage. A Carl Zeiss optical polarizing microscope equipped with a Mettler FP82HT hot stage and a Mettler FP90 central processor was used to evaluate the homogeneity and the homeotropic alignment of the specimens and to determine the nematic-to-isotropic transition temperatures, $T_{NI}$, of the samples at a cooling rate of 2 °C/min. The $T_{NI}$ of the mixtures refers to the lower bound of the narrow biphasic region. Typically, the transition zone for the SCLCP/nematic mixtures was in a range of 1−3 °C. The $T_{NI}$ values of the mixtures were found to be slightly higher than that of 5OCB (1−1.5 °C), varying slightly with DP, $n$, and the polymer concentration. Also, the refractive indices of the SCLCP mixtures can safely be assumed to be equal to that of pure 5OCB because the polymer concentrations utilized are very dilute.[2]

**Electric-Field-Dependent Dynamic Light Scattering.** The methodological and analytical procedures for the determination of viscoelastic parameters via the application of dynamic light scattering can be found in detail elsewhere.[4,26−29] Dynamic light scattering measurements in the homodyne mode were performed using a photon correlation spectrometer comprising a 15 mW He−Ne linearly polarized laser and a Brookhaven Instruments BI-2030AT 264-channel digital correlator at measured temperatures of 52, 57, and 62 °C, respectively. The samples were sandwiched between two glass slides and positioned in a refractive index-matching bath containing *tert*-butylbenzene, controlled by a circulating bath to an accuracy of ±0.1 °C, using a custom-designed micromanipulator which enables a small adjustment to keep the scattering volume in the focal plane of the collecting lens. The incoming laser beam is normal to the cell surface so that the average director is parallel to the incident wave vector. The incident light is polarized perpendicular to the scattering plane, and depolarized scattered light is detected with its polarization in the scattering plane. For this circumstance, at small scattering angles, scattering from a pure twist distortion is observed with a negligible contribution from the bend mode because of the large value of the ratio $q_\perp^2/q_{||}^2$, where $q_{||}$ and $q_\perp$ are, respectively, the components of the scattering vector parallel and perpendicular to the director. For example, at scattering angle of 18° in the laboratory frame, $q_\perp^2/q_{||}^2 = 142$, 113, and 85 for pure 5OCB at 52, 57, and 62 °C, respectively; hence, the contribution of the bend mode to the relaxation rate $\Gamma_2$ (i.e., bend−twist mode 2) is comparable to experimental error, which is about 2%.[4,7]

Individual values of the twist viscosity coefficient ($\gamma_1$) and elastic constant ($K_{22}$) can be acquired by carrying out the DLS measurement at small angles in the presence of an electric field parallel to the director. This technique leads to the following decay rate[26,28]

$$\Gamma_2(q) = \frac{K_{22}q_\perp^2}{\gamma_1} + \frac{\epsilon_0\Delta\epsilon\left(\frac{V}{d}\right)^2}{\gamma_1} \tag{15}$$

and

$$q_\perp = \left(\frac{2\pi n_e}{\lambda}\right)\sin\theta_0 \tag{15a}$$

where $q_\perp$ is the scattering vector perpendicular to the nematic director; $n_e$ is the temperature-dependent extraordinary refractive index of the nematic; $\lambda$ is the wavelength of incident light in a vacuum (632.8 nm); $\theta_0$ refers to the scattering angle inside the nematic sample and can be calculated by Snell's law, viz., $n_e \sin\theta_0 = n_T \sin\theta_{lab}$, where $n_T$ is the refractive index of *tert*-butylbenzene, used as matching liquid, and $\theta_{lab}$ is the scattering angle in the laboratory frame (i.e., the angle between the transmitted laser beam and the photomultiplier tube); $V$ is the applied voltage across the sample cell; $d$ is the cell thickness; $\epsilon_o$ is the electric permittivity in a vacuum; and $\Delta\epsilon$ is the dielectric anisotropy of the liquid crystalline solution. In EFDLS measurements, the depolarized intensity correlation functions of each specimen were obtained by photon correlation analysis with each level of AC electric field applied by a Hewlett-Packard audio frequency generator model 200CDR at 6000 Hz. Further details of the experimental method can be found elsewhere.[7,10,11] The concentration dependence of $\gamma_1$ was found to be a linear function of concentration up to 0.03 g/mL in agreement with previous studies.[10,12] Therefore, measurements to compare the effect of LCP structure on twist viscosity increment were made on 0.03 g/mL solutions.

**Table 2. Dielectric Anisotropies ($\Delta\epsilon$) and Threshold Voltages ($V_{th}$) of Pure 5OCB and SCLCP/5OCB Solutions ($c$ = 0.03 g/mL)**

| | $\Delta\epsilon$ (±3%) | | | $V_{th}$ (±2%) | | |
|---|---|---|---|---|---|---|
| sample | 62 °C | 57 °C | 52 °C | 62 °C | 57 °C | 52 °C |
| 5OCB | 10.20 | 11.28 | 12.69 | 0.64 | 0.69 | 0.72 |
| no. 1 | 8.94 | 10.00 | 11.32 | 0.64 | 0.66 | 0.71 |
| no. 2 | 9.18 | 10.25 | 11.43 | 0.64 | 0.66 | 0.70 |
| no. 3 | 8.99 | 10.59 | 11.81 | 0.65 | 0.66 | 0.70 |
| no. 4 | 8.91 | 10.24 | 11.53 | 0.65 | 0.66 | 0.69 |
| no. 5 | 8.97 | 10.37 | 11.93 | 0.65 | 0.66 | 0.70 |

**Freedericksz Transition Measurement.** The dielectric anisotropy, $\Delta\epsilon$ ($=\epsilon_{\parallel} - \epsilon_{\perp}$), and the threshold voltage, $V_{th}$, of the LCP samples were determined via the Freedericksz transition technique. This method also yields a determination of the splay elastic constant, $K_{11}$, and is described in detail elsewhere.[30,31] Basically, this measurement involves monitoring the capacitance of a planar monodomain while an increasing bias voltage ($V_b$) is applied. A three-terminal arrangement with guard electrodes was used to eliminate edge effects. $K_{11}$ can be calculated via following expression:[30]

$$V_{th}^2 = \frac{K_{11}\pi^2}{\epsilon_0 \Delta\epsilon} \tag{16}$$

The value of $\epsilon_{\perp}$ was measured at zero field for a planar monodomain, neglecting the capacitance contribution from the polyimide, and the value of $\epsilon_{\parallel}$ was determined by measuring the capacitance of the homeotropic cell in the presence of a 7 V 3000 Hz AC bias voltage frequency. The details of the method are given elsewhere.[7,31]

**Rheological Analysis.** ER measurements were made with a Carrimed controlled-stress rheometer equipped with a cone-and-plate fixture, which also functions as electrodes. Application of a DC voltage across the gap, i.e., in the direction perpendicular to the shear flow, was executed through mercury by a Bertan model 215 high-voltage power supply. The gap can be adjusted very precisely using the conductance of the cone-and-plate disk. Because the cone angle is 0.5° and the diameter is 2 cm, the magnitude of the electric field varies radially in this geometry, being smallest at the edge and largest at the tip. For example, with a gap at the tip of 15 $\mu$m, the average value of the applied field is 2.2 kV/mm at 100 V, determined to be a saturation field in previous works.[19,20] Hence, the apparent viscosity at this field is only weakly dependent on the applied voltage at a low shear stress and decreases slowly with shear stress. In this work, the stress sweep method[19,20] was performed to measure the Miesowicz viscosity $\eta_c$, where the director is pinned perpendicular to the flow direction,[21] by extrapolation of $\eta_{on}$ to zero shear under a saturation field.[12,19,20] The sample temperature was controlled by a water pump circulation system accurate to within ±0.1 °C. To achieve uniform temperature throughout the gap, the samples were equilibrated at temperature for 10 min.

## Results and Discussion

Measurements of the mean twist relaxation rates, based on single-exponential fits to the autocorrelation function of light scattered by dilute nematic solutions of SCLCPs in 5OCB, were carried out using the twist scattering configuration described above. To carry out EFDLS analysis, we first determined the values of dielectric anisotropy, $\Delta\epsilon$, and the threshold voltage, $V_{th}$, from Freedericksz transition measurement for pure 5OCB as well as for the nematic solutions of SCLCPs as listed in Table 2. Note that, in comparison with pure 5OCB, the $\Delta\epsilon$ values of the polymer solutions are slightly smaller, consistent with the values of a previous study,[31] indicating that the local order parameter decreases with addition of LCP into the nematic matrix. In addition, at lower temperatures, $\Delta\epsilon$ increases for all samples, which reflects the higher nematic order in the system.[29] Further, we compute the splay elastic constant, $K_{11}$, from eq 16, using the measured $\Delta\epsilon$ and $V_{th}$ values. The results are shown in Table 3 and indicate, first, good agreement with the earlier data of Bradshaw[32] listed in parentheses and, further, that $K_{11}$ decreases slightly with dissolution of side-chain liquid crystalline polysiloxanes, in agreement with literature observation in other solvents.[4,31,33] Table 3 shows that $K_{11}$ is not dependent significantly on DP or spacer length at a specified temperature.

**Table 3. Splay Elastic Constants of Pure 5OCB and SCLCP/5OCB Solutions ($c$ = 0.03 g/mL)**

| | ($K_{11}$ ± 5%) × $10^{-8}$ (dyne) | | |
|---|---|---|---|
| sample | 62 °C | 57 °C | 52 °C |
| 5OCB | 38.55 (37.50) | 48.57 (49.00) | 58.35 (58.00) |
| no. 1 | 32.86 | 39.09 | 50.60 |
| no. 2 | 33.74 | 39.81 | 50.67 |
| no. 3 | 33.95 | 40.99 | 51.93 |
| no. 4 | 33.26 | 40.38 | 49.68 |
| no. 5 | 34.10 | 41.74 | 52.87 |

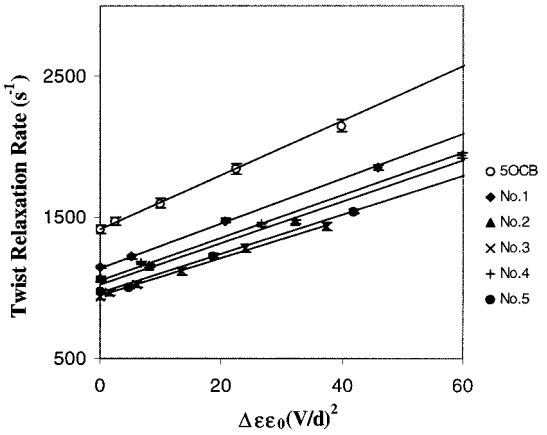


**Figure 2.** Electric field dependence of the twist relaxation rates for pure 5OCB and SCLCP/5OCB mixtures ($c$ = 0.03 g/mL) at 52 °C.

**Table 4. Twist Viscosity, $\gamma_1$, and Twist Elastic Constant, $K_{22}$, of Pure 5OCB and SCLCP/5OCB Solutions ($c$ = 0.03 g/mL)**

| | $\gamma_1$ ± 1% (poise) | | | ($K_{22}$ ± 2%) × $10^{-8}$ (dyne) | | |
|---|---|---|---|---|---|---|
| sample | 62 °C | 57 °C | 52 °C | 62 °C | 57 °C | 52 °C |
| 5OCB | 0.24 | 0.34 | 0.52 | 23.18 | 29.01 | 35.46 |
| no. 1 | 0.31 | 0.45 | 0.63 | 23.85 | 29.65 | 34.92 |
| no. 2 | 0.34 | 0.49 | 0.68 | 23.56 | 28.93 | 33.95 |
| no. 3 | 0.36 | 0.52 | 0.75 | 23.48 | 29.26 | 34.41 |
| no. 4 | 0.32 | 0.46 | 0.66 | 23.51 | 28.72 | 34.17 |
| no. 5 | 0.36 | 0.51 | 0.73 | 22.48 | 28.66 | 34.19 |

In photon correlation spectroscopy, previous work has shown that a decrease in twist relaxation rates in EFDLS occurs on dissolution of an LCP in an LMMN solvent that is basically due to a combination of a large increase in $\gamma_1$ and a small change in $K_{22}$. As can be seen in Figure 2, the relaxation rates of the twist mode of pure 5OCB and SCLCP/5OCB solutions were found to increase linearly with the field parameter $\epsilon_0\Delta\epsilon(V/d)^2$, in agreement with eq 15. Table 4 lists the values of $\gamma_1$ and $K_{22}$ obtained, respectively, from the inverse slope and the intercept, corresponding to the zero-field decay rate, through least-squares fits to eq 15. These results show that, in qualitative agreement with literature,[8] the $K_{22}$

**Table 5. Viscosity Increments $\delta\gamma_1/c$, $\delta\eta_{on}/c$, and $\delta\eta_{off}/c$ of SCLCP/5OCB Solutions ($c$ = 0.03 g/mL)**

| | | | $(\delta\gamma_1/c)^a \pm 4\%$ | | | $(\delta\eta_{on}/c)^b \pm 4\%$ | | | $(\delta\eta_{off}/c)^b \pm 4\%$ | | |
|---|---|---|---|---|---|---|---|---|---|---|---|
| sample | DP | $n$ | 62 °C | 57 °C | 52 °C | 62 °C | 57 °C | 52 °C | 62 °C | 57 °C | 52 °C |
| no. 1 | 45 | 3 | 2.60 | 3.53 | 3.80 | 3.15 | 4.57 | 4.91 | 2.28 | 3.11 | 3.52 |
| no. 2 | 72 | 3 | 3.53 | 4.87 | 5.53 | 3.27 | 4.66 | | 3.08 | 4.00 | |
| no. 3 | 198 | 3 | 4.13 | 6.00 | 7.76 | 3.52 | 5.22 | 6.56 | 4.42 | 5.84 | 6.11 |
| no. 4 | 198 | 5 | 2.90 | 3.97 | 4.93 | 3.67 | 5.09 | | 2.95 | 4.06 | |
| no. 5 | 198 | 11 | 3.97 | 5.67 | 7.03 | 3.85 | 4.83 | 6.98 | 3.92 | 5.07 | 7.30 |

[a] The data obtained from EFDLS measurement in this work. [b] The data obtained from ER measurement (samples no. 1−4 taken from Yao and Jamieson,[12] whereas sample no. 5 was measured in this work).

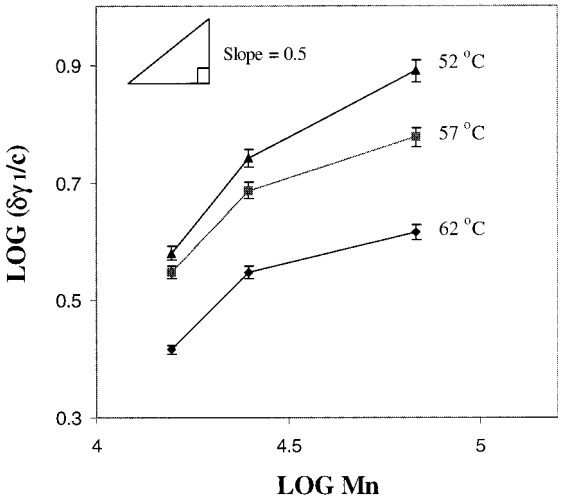


**Figure 3.** Molecular weight dependence of the reduced viscosity increment $\delta\gamma_1/c$ of the SCLCP/5OCB mixtures ($n$ = 3, $c$ = 0.03 g/mL). ($M_n$ is the true number-average molecular weight obtained via NMR analysis). Inset shows slope for nondraining Gaussian coil ($\delta\eta/c \approx M^{0.5}$).

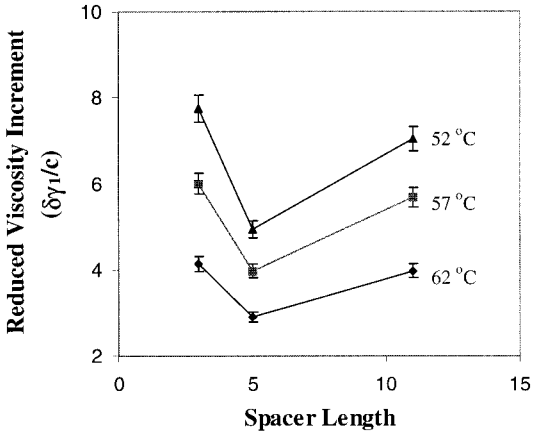


**Figure 4.** Spacer length dependence of the reduced viscosity increment $\delta\gamma_1/c$ of the SCLCP/5OCB mixtures (DP = 198, $c$ = 0.03 g/mL).

values of a 0.03 g/mL SCLCP solution are comparable to that of pure 5OCB, whereas $\gamma_1$ values for the mixtures increase substantially. Hence, it is evident that the change in $K_{22}/\gamma_1$ is dominated by an increase in $\gamma_1$. The fact that, in Table 4, there is a clear increase in $\gamma_1$ for all of the SCLCP/5OCB mixtures is significant, because the ER results of Yao and Jamieson[12,22] suggest that, for these SCLCP, $R_{||} \approx R_\perp$. Hence, a substantial increase in $\gamma_1$ is inconsistent with the original Brochard theory (eq 1), which indicates $\delta\gamma_1 \approx 0$ if $R_{||} \approx R_\perp$. Thus, the finite twist viscosity increment of SCLCP/5OCB solutions further supports that the original Brochard theory needs to be modified.

Table 5 compares the reduced viscosity increments $\delta\gamma_1/c$, $\delta\eta_{on}/c$, and $\delta\eta_{off}/c$ of the nematic mixtures at three different temperatures. Here, $\delta\eta_{on} = \eta_{on} - \eta_{on}^0$ and $\delta\eta_{off} = \eta_{off} - \eta_{off}^0$ (where $\delta\eta_{on}$ and $\delta\eta_{off}$, respectively, refer to the viscosity increments determined with the electric field on and off in the ER measurement; $\eta$ and $\eta^0$ signify the viscosity coefficients of solution and pure solvent, respectively); $c$ is the polymer concentration (g/mL). The $\delta\gamma_1/c$ values were measured by EFDLS in this work, whereas the values of $\delta\eta_{on}/c$ and $\delta\eta_{off}/c$ were taken from the very recent study of Yao and Jamieson,[12] except for sample no. 5 (DP = 198, $n$ = 11), for which all three viscosity increments were measured in this study. It can be seen in Table 5 that all three viscosity increments become larger at lower temperatures, which primarily reflects an increase in the conformational relaxation time, $\tau_R$, cf. eqs 1−7 and 12−14.

Figure 3 shows the dependence of the twist viscosity increment $\delta\gamma_1$ on the molecular weight for spacer length $n$ = 3. Evidently, from Figure 3, we see that $\delta\gamma_1/c$ increases significantly with molecular weight. These results can be compared with our earlier ER observations.[12] At fixed spacer length $n$ = 3, 5, and 11 and at a constant temperature in the nematic state, we observed that $\delta\eta_{off}/c$ has a noticeable molecular weight dependence comparable to that seen here for $\delta\gamma_1/c$, whereas the molecular weight dependence of $\delta\eta_{on}/c$ is negligible. This was interpreted[12] on the basis of the Brochard model (eqs 6 and 7), again equating $\delta\eta_{on} = \delta\eta_c$ and $\delta\eta_{off} = \delta\eta_b$, as due to the fact that, whereas $\tau_R$ increases with molecular weight, this is accompanied by a decrease in the ratio $R_{||}/R_\perp$. As indicated in Figure 3, the molecular weight dependence measured for $\delta\gamma_1/c$ is comparable to that for a Gaussian random coil ($\delta\eta/c \approx M^{0.5}$) at low molecular weights but is weaker than random coil at higher molecular weights.

Figure 4 exhibits the variation in $\delta\gamma_1$ with spacer length at constant DP = 198. We find from Figure 4 that there is a minimum in $\delta\gamma_1/c$ at $n$ = 5. Moreover, compared with our earlier ER data, at fixed DP, a minimum in $\delta\eta_{off}/c$ was found in the previous work,[12] whereas in contrast, $\delta\eta_{on}/c$ showed no change with spacer length. Again, this earlier result was interpreted,[12] via the Brochard model, that the change in spacer length results in changes in $\tau_R$ and $R_{||}/R_\perp$ in opposite directions, viz., a minimum in $\tau_R$ at $n$ = 5, and a maximum in $R_{||}/R_\perp$.

Alternatively, as previously pointed out,[12] the variations in a particular viscosity increment $\delta\eta$ can be expressed in terms of corresponding differences in the effective hydrodynamic volume via Einstein's relationship, i.e., $[\eta] = \delta\eta/\eta^0\ c = 2.5N_AV_h^{eff}/M$, where $N_A$ is Avogadro's number, $V_h^{eff}$ is the effective hydrodynamic volume of the polymer, and $M$ is the true molecular weight of a polymer obtained by NMR data, listed in Table 1. Thus, Figure 4 and Table 5 imply that $V_h^{eff}$ in the nematic state, for both $\delta\gamma_1$ and $\delta\eta_{off}$, has a minimum

**Table 6. Chain Anisotropy ($R_\perp/R_\parallel$) of SCLCP/5OCB Solutions ($c$ = 0.03 g/mL)**

| | | | Brochard model $(\delta\gamma_1/\delta\eta_c)^a$ $(R_\perp/R_\parallel) \pm 3\%$ | | | modified model $(\delta\gamma_1{}^{\text{modified}}/\delta\eta_c)^b$ $(R_\perp/R_\parallel) \pm 3\%$ | | | ER $(\delta\eta_b/\delta\eta_c)^c$ $(R_\perp/R_\parallel) \pm 2\%$ | | |
|---|---|---|---|---|---|---|---|---|---|---|---|
| sample | DP | n | 62 °C | 57 °C | 52 °C | 62 °C | 57 °C | 52 °C | 62 °C | 57 °C | 52 °C |
| no. 1 | 45 | 3 | 1.38 | 1.37 | 1.37 | 0.88 | 0.81 | 0.81 | 0.93 | 0.91 | 0.92 |
| no. 2 | 72 | 3 | 1.43 | 1.42 | | 1.04 | 1.02 | | 0.99 | 0.96 | |
| no. 3 | 198 | 3 | 1.44 | 1.44 | 1.44 | 1.07 | 1.06 | 1.08 | 1.06 | 1.03 | 0.98 |
| no. 4 | 198 | 5 | 1.37 | 1.37 | | 0.84 | 0.82 | | 0.95 | 0.95 | |
| no. 5 | 198 | 11 | 1.42 | 1.44 | 1.42 | 1.02 | 1.07 | 1.01 | 1.01 | 1.02 | 1.01 |

[a] Equation 17. [b] Equation 18. [c] Equation 8.

at $n = 5$ consistent with that observed in GPC analysis.[12] Such a minimum is not seen in the hydrodynamic volume from $\delta\eta_{on}$.

To summarize, we have generated new results on the increment in twist viscosity of SCLCP solutions which we compare with previous ER measurements of the increments $\delta\eta_{on}$ and $\delta\eta_{off}$. We find that $\delta\gamma_1$ and $\delta\eta_{off}$ increase substantially with molecular weight and show a minimum at spacer length $n = 5$. In contrast, $\delta\eta_{on}$ increases very weakly with molecular weight and shows no detectable minimum at $n = 5$.

The question now arises: can we consistently interpret these experimental results in terms of the molecular chain conformation? To explain the ER data, we again employ eq 8 of Brochard[1], identifying $\eta_{on}$ and $\eta_{off}$ with the Miesowicz viscosities $\eta_c$ and $\eta_b$, respectively, that is, $\eta_c = \eta_{on}$ and $\eta_b = \eta_{off}$. Also, combination of eqs 1 and 7 of Brochard[1] leads to

$$\frac{\delta\gamma_1}{\delta\eta_c} = \left(\frac{R_\perp^2}{R_\parallel^2} - 1\right)^2 \tag{17}$$

However, as noted above, previous work has led us to modify the results of Brochard for the rotational viscosity $\delta\gamma_1$. Thus, combining the modified result, eq 10, with eq 7, we obtain a different expression for the ratio of viscosity increments:

$$\left(\frac{\delta\gamma_1^{\text{modified}}}{\delta\eta_c}\right) = \frac{R_\perp^4}{R_\parallel^4} - \frac{R_\perp^2}{R_\parallel^2} + 1 \tag{18}$$

Equations 8 and 17 from Brochard's model and eqs 8 and 18 from our modified theory provide alternative possibilities to obtain a consistent interpretation of ER behavior ($\delta\eta_b$ and $\delta\eta_c$) and EFDLS ($\delta\gamma_1$). Table 6 shows the conformational anisotropy ($R_\perp/R_\parallel$) of the SCLCPs at three different temperatures, calculated from eqs 8, 17, and 18. Clearly, the values obtained from ratio $\delta\gamma_1{}^{\text{modified}}/\delta\eta_c$ via eq 18 are in better agreement with those deduced from the ER data via eq 8 than values obtained from the original Brochard[1] prediction (eq 17).

It should be further apparent, from eqs 7 and 12, that, knowing $R_\parallel/R_\perp$, we can proceed to determine the conformational relaxation time, $\tau_R$. In Figure 5, we plot values of the conformational relaxation time $\tau_R$ for SCLCP samples with $n = 3$ and varying DP in 5OCB at 57 and 62 °C. We also plot in Figure 5 estimated values of $\tau_R$ for the SCLCP in the GPC solvent, tetrahydrafuran (THF), at 30 °C, computed from the GPC hydrodynamic volumes $V_h$ via[34]

$$\tau_R = \frac{3\eta_s V_h}{kT} \tag{19}$$

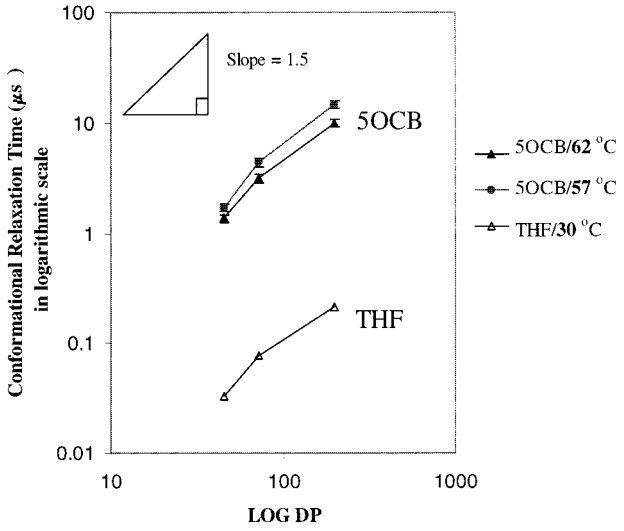


**Figure 5.** DP dependence of the conformational relaxation time ($\tau_R$, $\mu$s) of SCLCPs ($n = 3$) in 5OCB (● at 57 °C and ▲ at 62 °C) and in THF (△ at 30 °C, calculated from GPC hydrodynamic volume). Inset shows slope for nondraining Gaussian coil ($\tau_R \approx N\delta\eta/(ckT) \approx M^{1.5}$).

where $\eta_s$ is the viscosity of THF; $k$ is Boltzmann's constant, and $T$ is the absolute temperature of the GPC experiment (303 K). $V_h$ is computed from the weight-average polystyrene-equivalent molecular weights (Table 1) using

$$M_w[\eta] = 2.5N_A V_h \tag{20}$$

and the Mark−Houwink relation of Appelt and Meyerhoff[35] for polystyrene in THF

$$[\eta] = 1.363 \times 10^{-2} M_w{}^{0.714} \tag{21}$$

The results shown in Figure 5 indicate that the $\tau_R$ values extracted from the viscometric data in nematic 5OCB are larger than those in isotropic THF computed from the GPC hydrodynamic volumes by a factor of approximately 50 times. However, this difference is drastically reduced to approximately 0.7 times, when the $\tau_R$ values are corrected via eq 19 for the difference in temperature and medium viscosity (57 °C in 5OCB vs 30 °C in THF, and $\gamma_1$ (5OCB) = 0.34 poise vs $\eta$ (THF) = 0.0044 poise). Thus, the molecular hydrodynamic volume of the SCLCP in nematic 5OCB is numerically comparable (approximately 30% smaller) to its value in isotropic THF. The residual discrepancy may represent conformational differences associated with nematic ordering in 5OCB or differences in excluded volume between the two solvent systems. It is further evident in Figure 5 that the molecular weight dependence of $\tau_R$, and hence that of the hydrodynamic volume, is analo-

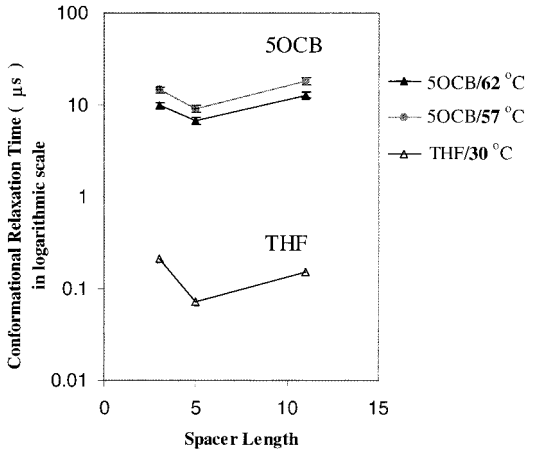


**Figure 6.** Spacer length dependence of the conformational relaxation time ($\tau_R$, $\mu$s) of SCLCPs (DP = 198) in 5OCB (● at 57 °C and ▲ at 62 °C) and in THF (△ at 30 °C, calculated from GPC hydrodynamic volume).

gous in 5OCB and THF and similar to that ($\tau_R \approx N^{1.5}$) for a Gaussian random coil.

Next, in Figure 6, we plot the $\tau_R$ values in 5OCB for SCLCP with DP = 198 and varying spacer lengths, together with values estimated in THF from eqs 19−21. Again, good agreement is found between each set of values when corrected for the difference in temperature and medium viscosity. At each spacer length, the hydrodynamic volume of the SCLCP is comparable in both 5OCB and THF, and each exhibits a minimum value at spacer length $n = 5$. The modified hydrodynamic model of Brochard, embodied in eqs 6, 7, and 12, thus produces a consistent interpretation of all three viscosity increments of the SCLCP in nematic 5OCB, $\delta\eta_{on} = \delta\eta_c$, $\delta\eta_{off} \approx \delta\eta_b$ and $\delta\gamma_1$. The stronger molecular weight dependence of $\delta\eta_{off}$ and $\delta\gamma_1$ relative to that of $\delta\eta_{on}$ derives from an increase in $\tau_R$ coupled to an increase in $R_\perp/R_\parallel$ with molecular weight (Table 6). The minimum in $\delta\eta_{off}$ and $\delta\gamma_1$, together with invariance of $\delta\eta_{on}$ as spacer length is varied through $n = 3$, 5, and 11, reflects the minimum in $\tau_R$ coupled to a minimum in $R_\perp/R_\parallel$ at $n = 5$.

The minimum in hydrodynamic volume at $n = 5$ with fixed DP is observed both in nematic 5OCB and in isotropic THF. Its origin could arise from a minimum in molecular weight (e.g., from insufficient substitution by mesogenic side chains) or from a more compact chain conformation. On the basis of our previous finding[12] that all polymers have a comparable degree of substitution, we favor the latter interpretation. Thus, we infer that the decrease in $V_h$ on increasing spacer length from $n = 3$ to 5 reflects an increase in backbone flexibility. The increase in $V_h$ accompanying the increase in spacer length from $n = 5$ to 11 may be due to the added volume from the longer spacer. The viscometric data in 5OCB indicates further (Table 6) that, for the polymer with DP = 198, a change in shape from oblate ($n = 3$) to prolate ($n = 5$) and back to oblate ($n = 11$) occurs in the nematic state. We note that, whereas in the pure SCLCP, polymers with shorter spacers ($n = 3$ and 5) form only nematic phases, the SCLCP with largest spacer ($n = 11$) forms smectic phases, which is generally accompanied by microsegregation of the spacers and backbone into layers, and leads to an oblate conformation.[36,37]

## Conclusions

The viscoelastic behavior of the twist distortion was investigated via the technique of electric-field-dependent dynamic light scattering for a series of side-chain LCPs in 5OCB nematic solvent as a function of temperature, molecular weight, and spacer length. Specifically, it was observed that dissolution of a side-chain LCP produces a substantial increase in the twist viscosity coefficient, $\gamma_1$, and only a very small change in twist elastic constant, $K_{22}$. We found further that the increment $\delta\gamma_1$ of SCLCP specimens varies with spacer length and molecular weight, proportional to changes in the molecular hydrodynamic volume of the polymer, as predicted by the hydrodynamic theory of Brochard when modified to include an additional viscous dissipation due to an elastic coupling between director rotation and the orientation of LCP.

**Acknowledgment.** We gratefully thank Mr. Doug Bryant at Kent State University for preparation of polyimide and ITO-coated glass slides and NSF Grant DMR 89-20147 for financial support.

## References and Notes

(1) Brochard, F. *J. Polym. Sci., Polym. Phys. Ed.* **1979**, *17*, 1367.
(2) Mattoussi, H.; Ober, R. *Macromolecules* **1990**, *23*, 1809.
(3) Mattoussi, H.; Veyssie, M. *J. Phys.* **1989**, *50*, 99.
(4) Gu, D.-F.; Jamieson, A. M.; Rosenblatt, C.; Tomazos, D.; Lee, M.; Percec, V. *Macromolecules* **1991**, *24*, 2385.
(5) Weill, C.; Casagrande, C.; Veyssie, M. *J. Phys. II* **1986**, *47*, 887.
(6) Pashkovsky, E. E.; Litvina, T. G.; Kostromin, S.; Shibaev, V. P. *J. Phys. II* **1992**, *2*, 1577.
(7) Gu, D.-F.; Jamieson, A. M.; Lee, M.; Kawasumi, M.; Percec, V. *Liq. Cryst.* **1992**, *12*, 961.
(8) Coles, H. J.; Sefton, M. S. *Mol. Cryst. Liq. Cryst., Lett. Sect.* **1985**, *1*, 159.
(9) Gu, D.-F.; Jamieson, A. M.; Lee, M.; Kawasumi, M.; Percec, V. *Macromolecules* **1992**, *25*, 2151.
(10) Chen, F.-L.; Jamieson, A. M. *Macromolecules* **1994**, *27*, 1943.
(11) Chen, F.-L.; Jamieson, A. M.; Kawasumi, M.; Percec, V. *J. Polym. Sci., Polym. Phys.* **1995**, *33*, 1213.
(12) Yao, N.; Jamieson, A. M. *Macromolecules* **1997**, *30*, 5822.
(13) Gu, D.-F.; Jamieson, A. M.; Wang, S. Q. *J. Rheol.* **1993**, *37*, 985.
(14) Gu, D.-F.; Jamieson, A. M. *Macromolecules* **1994**, *27*, 337.
(15) Yao, N.; Jamieson, A. M. *J. Rheol.* **1998**, *42*, 603.
(16) de Gennes, P.-G.; Prost, J. *The Physics of Liquid Crystals*, 2nd Ed.; Claredon Press: Oxford, U.K., 1993.
(17) Jamieson, A. M.; Gu, D.-F.; Chen, F.-L.; Smith, S. *Prog. Polym. Sci.* **1996**, *21*, 981.
(18) Gu, D.-F.; Jamieson, A. M. *J. Rheol.* **1994**, *38*, 555.
(19) Chiang, Y.-C.; Jamieson, A. M.; Kawasumi, M.; Percec, V. *Macromolecules* **1997**, *30*, 1992.
(20) Chiang, Y.-C.; Jamieson, A. M.; Campbell, S.; Lin, Y.; O'Sidocky, N.; Chen, L.-C.; Kawasumi, M.; Percec, V. *Rheol. Acta* **1997**, *36*, 505.
(21) Skarp, K.; Lagerwall, S. T.; Stebler, B. *Mol. Cryst. Liq. Cryst.* **1980**, *60*, 215.
(22) Yao, N.; Jamieson, A. M. *Macromolecules* **1998**, *31*, 5399.
(23) Williams, D. R. M.; Halperin, A. *Macromolecules* **1993**, *26*, 2025.
(24) Chen, F.-L. Ph.D. Thesis, Case Western Reserve University, Cleveland, OH, 1994.
(25) Kinzer, D. *Mol. Cryst. Liq. Cryst., Lett. Sect.* **1985**, *1*, 147.
(26) Orsay Liquid Crystal Group. *J. Chem. Phys.* **1969**, *51*, 816.
(27) Orsay Liquid Crystal Group. *Phys. Rev. Lett.* **1969**, *22*, 1361.
(28) Leslie, F. M.; Waters, C. M. *Mol. Cryst. Liq. Cryst.* **1985**, *123*, 101.
(29) Sefton, M. S.; Bowdler, A. R.; Coles, H. J. *Mol. Cryst. Liq. Cryst.* **1985**, *129*, 1.
(30) Meyerhofer, D. *J. Appl. Phys.* **1975**, *46*, 5084.
(31) Gu, D.-F.; Smith, S. R.; Jamieson, A. M.; Lee, M.; Percec, V. *J Phys. II* **1993**, *3*, 937.

(32) Bradshaw, M. J.; Raynes, E. P.; Bunning, J. D.; Faber, T. E. *J. Phys.* **1985**, *46*, 1513.
(33) Coles, H. J.; Hopwood, A. I. *Mol. Cryst. Liq. Cryst., Lett. Sect.* **1985**, *1*, 165.
(34) Tanford, C. *Physical Chemistry of Macromolecules*; John Wiley & Sons: New York, 1961.
(35) Appelt, B.; Meyerhoff, G. *Macromolecules* **1980**, *13*, 657.
(36) Pépy, G.; Noirez, L.; Keller, P.; Lambert, M.; Moussa, F.; Cotton, J. P. *Makromol. Chem.* **1990**, *191*, 1383.
(37) Fourmaux-Demange, V.; Boué, F.; Brûlet, A.; Keller, P.; Cotton, J. P. *Macromolecules* **1998**, *31*, 801.

MA990389E